

Non-universal BCS-BEC crossover in resonantly interacting Fermi gases

L. M. Jensen^{1,2}

¹*NORDITA, Blegdamsvej 17, DK-2100, Copenhagen Ø, Denmark*

²*Department of Theoretical Physics, Umeå University, 901 87, Umeå, Sweden**

We investigate the non-universal behavior of the BCS-BEC crossover model at the normal to superfluid transition. By using a finite temperature quantum field theoretical approach due to Nozières and Schmitt-Rink and by making the effective range expansion of the effective two-body interaction we numerically calculate the crossover transition temperature as a function of the scattering length, a_F , and the effective range parameter, r_e . In an ultracold two-component atomic Fermi gas BCS-BEC crossover physics is expected to appear near magnetic-field-induced Feshbach resonances. By matching two-body scattering properties near a Feshbach resonance to a simple renormalized model potential, a broad resonance is characterized by a small effective range and the gas displays a universal BCS-BEC crossover behavior. On the other hand, for a narrow resonance thermodynamic quantities depend the effective range which may be large and negative at resonance. For increasing values of $-r_e$ we find the transition temperature to be suppressed in the crossover region. We furthermore argue for existence of a lower bound of T_c at fixed coupling for increasing $-r_e$ in the crossover region.

PACS numbers: 03.75.Ss, 03.75.Hh, 05.30.Jp

I. INTRODUCTION

The prospect of creating a fermion superfluid in trapped atomic Fermi gases using a magnetic field induced Feshbach resonance has received much experimental and theoretical attention in the past year. Recently long-lived diatomic molecules of fermionic ${}^6\text{Li}$ and ${}^{40}\text{K}$ [1, 2, 3], Bose-Einstein condensation (BEC) of molecular ${}^6\text{Li}_2$ and ${}^{40}\text{K}_2$ dimers [4, 5, 6], crossover from a molecular BEC to a degenerate and strongly interacting Fermi gas [7, 8], and condensation of fermionic atom pairs [9, 10] have been reported. From measurements of the energy gaps in the excitation spectrum [11, 12] and of the frequencies and damping of compressional collective modes as a function of the effective atom-atom interaction [8, 13] evidence is emerging that some of the experiments are already probing the superfluid phase.

From a theoretical point of view the low temperature atom gases with resonant interactions have on the one hand been described in terms of coupled boson-fermion models where the atomic and molecular degrees of freedom have been treated separately but constrained by total fermion number conservation. On the other hand, the description of superfluid pairing in Fermi systems with a varying coupling constant has also been analyzed using a generalized Bardeen-Cooper-Schrieffer (BCS) variational function at zero temperature [14] and by Green's function methods at nonzero temperatures [15, 16] including explicitly only the fermionic degrees of freedom. In the latter approach a boson-like two-body bound state is formed at large couplings and the system displays a smooth transition from a gas of fermions which undergoes a phase transition to a BCS superfluid to a gas of

bosons which condenses at the Bose-Einstein condensation temperature.

In [17, 18, 19] it was argued that the universal crossover model based on a static contact potential applies only to broad Feshbach resonances, and that for more general potentials (*e.g.*, potentials characterized by the presence of a repulsive barrier) the solutions to the crossover equations depend sensitively on the effective range, which gives a measure of the energy dependence of the scattering phase shift and transition matrix. Similar conclusions were drawn in [20] based on a microscopic five coupled channels calculation of diatomic ${}^6\text{Li}$. In this study the molecular Born-Oppenheimer potentials were adjusted in order to reproduce the experimental resonance positions of the broad resonance at 822 G, the narrow resonance at 543G in addition to the zero crossing of the scattering length at 533 G and the hyperfine splitting between $F = 3/2$ and $F = 1/2$ states. The effective range was extracted and found to be small and positive for the broad resonance and thus consistent with the standard BCS-BEC crossover model. In contrast, the effective range for the narrow resonance was found to be large and negative. In relation to the two-channel scattering model derived from the boson-fermion models the relation between the effective range, r_e , at resonance and the boson-fermion coupling constant, g_{BF} , was found to be, $r_e = -8\pi\hbar^4/(m^2|g_{BF}|^2)$, where m is the mass of the atoms and when neglecting the background scattering length [18].

In the present work we generalize the calculation of the BCS-BEC crossover transition temperature to potential models with nonzero effective range. The paper is organized as follows: Section II contains a description of the finite temperature Green's function formalism [15] due to Nozières and Schmitt-Rink (NS). Partly following [21] the thermodynamic equations determining the transition temperature and chemical potential are presented, and

*Electronic address: melwyn@nordita.dk

the renormalization of the T-matrix equation including the effective range expansion of the effective interaction is explained. In Section III the resulting equations are numerically solved to determine the critical chemical potential and transition temperature in the crossover region as a functions of the effective range.

II. BCS-BEC CROSSOVER MODEL

The BCS-BEC crossover problem has a long history [14, 15, 16, 22] and it was recently revived in the context of high- T_c superconductivity of the cuprates. The generic crossover problem has also found applications in several other areas where pairing correlations are stronger than in the BCS theory, *e.g.*, the case of a strongly interacting Fermi gas with large scattering length. Let us consider the grand canonical Hamiltonian, $K = H - \mu N$, of a two-component atomic Fermi gas,

$$K = \sum_{\mathbf{k}, \sigma} \xi_{\mathbf{k}} a_{\mathbf{k}\sigma}^\dagger a_{\mathbf{k}\sigma} + \sum_{\mathbf{q}, \mathbf{k}, \mathbf{k}'} \frac{U_{\mathbf{k}\mathbf{k}'}}{\mathcal{V}} a_{\mathbf{k}+\frac{1}{2}\mathbf{q}\uparrow}^\dagger a_{-\mathbf{k}+\frac{1}{2}\mathbf{q}\downarrow}^\dagger a_{-\mathbf{k}'+\frac{1}{2}\mathbf{q}\downarrow} a_{\mathbf{k}'+\frac{1}{2}\mathbf{q}\uparrow}, \quad (1)$$

where $a_{\mathbf{k}\sigma}^\dagger, a_{\mathbf{k}\sigma}$ are the creation and annihilation operators for free atoms with momentum $\hbar\mathbf{k}$, energy $\varepsilon_{\mathbf{k}} = \hbar^2 k^2/2m$, the magnitude of the momentum $k = |\mathbf{k}|$, with the pseudospin index $\sigma = \uparrow, \downarrow$ denoting one of the two trapped hyperfine spin states, and with m and μ being the mass and chemical potential of the atoms, respectively. The single atom kinetic energy measured with respect to the chemical potential is $\xi_{\mathbf{k}} = \varepsilon_{\mathbf{k}} - \mu$, and the momentum dependent Fourier transform of the real space inter-atomic interaction is $U_{\mathbf{k}\mathbf{k}'} = U(|\mathbf{k} - \mathbf{k}'|)$ which in the crossover model with a bare attractive contact interaction has the constant strength, $U_{\mathbf{k}\mathbf{k}'} = U$. Due to the singular nature of the contact interaction unphysical divergences arise in three dimensions. The divergences may be removed by a standard regularization procedure [23]. By relating the bare potential to the two-body scattering length a_F and the corresponding effective strength, $U_* = 4\pi\hbar^2 a_F/m$, the bare potential can be eliminated in favor of the scattering length. This is formally accomplished by using the relation between bare and renormalized strengths, $U^{-1} = U_*^{-1} - \frac{1}{\mathcal{V}} \sum_{|\mathbf{k}| < k_c} (2\varepsilon_{\mathbf{k}})^{-1}$, where \mathcal{V} is the volume of the system, and $\hbar k_c$ is a momentum cutoff. At fixed a_F it is a relation between U and k_c . The final results become finite and k_c independent by taking the limit $k_c \rightarrow \infty$ at the end of the calculation. The $1/\varepsilon_{\mathbf{k}}$ term regulates the divergence of the free two-particle propagator. A similar procedure has been applied to the general case of model potentials with non-zero range and is presented in detail in the next section.

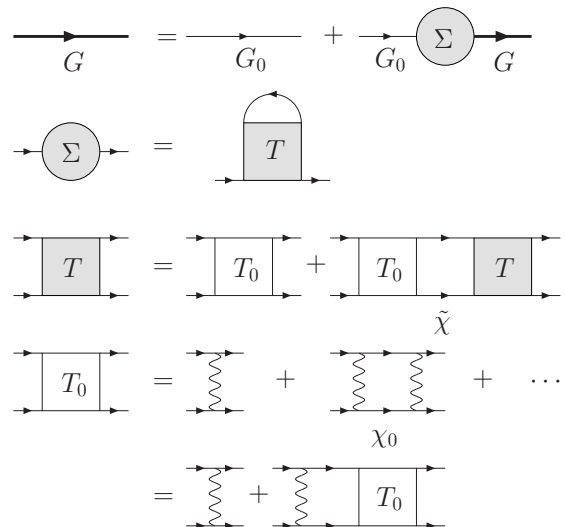


Figure 1: Diagrammatic structure of the equations for the dressed finite temperature propagator G (thick arrow lines). First line is the Dyson equation for the atomic propagator, the second line is the self-energy (shaded disc) derived from the T-matrix approximation, where the T-matrix (shaded square) is found from the integral equation in the third line. T_0 (white square) is the effective two-body interaction which is found after proper renormalization of the bare two-body interaction U (wiggly lines) by inverting the equation for T_0 in the fourth line. The non-interacting propagators are represented by the thin arrow lines, and the internal pair of fermions in the third and fourth lines are the regularized pair propagator, $\tilde{\chi}$, and non-interacting pair propagator, χ_0 , respectively.

A. Nonzero temperature Dyson equations

In the standard crossover model [14, 15, 16, 22] the BCS gap equation is supplemented by an equation for the number density. At fixed particle density this is an equation for the chemical potential, which in the BCS limit is the Fermi energy, $\mu \approx E_F$. In the BEC limit it is half of the bound state energy, $\mu = -E_0/2$, with $E_0 = \hbar^2/ma_F^2$. In the nonzero temperature Green's function formulation [15] of the crossover model the appearance of the bound states with finite center-of-mass momentum, \mathbf{q} , at sufficiently large interaction strength is accounted for by use of the T-matrix approximation for the self-energy. The T-matrix approximation diagrammatically corresponds to a resummation of an infinite series of particle-particle ladder diagrams. By using methods of nonzero temperature Green's function theory the equations for the transition temperature and critical chemical potential are derived from the corresponding Dyson equation within the T-matrix approximation,

$$G(\mathbf{k}, \omega_n) = G_0(\mathbf{k}, \omega_n) + G_0(\mathbf{k}, \omega_n) \Sigma(\mathbf{k}, \omega_n) G(\mathbf{k}, \omega_n), \quad (2)$$

with \mathbf{k} being an atomic wave-vector, $\omega_n = (2n+1)\pi/\beta$ is the fermionic Matsubara frequency for integer n , and where G_0 and G are the noninteracting and dressed finite

temperature Green's functions for the atoms, respectively (see Figure 1 for a diagrammatic representation). Unless specified we use below $\hbar = 1$, $k_B = 1$, and $\beta = 1/(k_B T)$ for the inverse temperature. The self-energy Σ is evaluated in the ladder approximation and is conveniently expressed in terms of the T-matrix which is the sum of ladder diagrams. In compact notation the equation for the many-body T-matrix T is $T = U + U\chi T$, where U is the momentum dependent bare interaction potential and χ is the in-medium pair propagator. The product $U\chi T$ is to be understood as a momenta convolutions. The convolutions will in general give rise to angular integrals. However, in relation to Feshbach resonances the important physics resides in the energy dependence of the T-matrix to which we make a low energy expansion. The angular integral can therefore be applied to the pair propagator alone and the angular dependence vanishes from the T-matrix equation. In general the T-matrix depends on the two incoming particle momenta, $\mathbf{k}_1, \mathbf{k}_2$ and two outgoing $\mathbf{k}'_1, \mathbf{k}'_2$. For the off-shell T-matrix there are in addition dependence on two incoming ω_1, ω_2 and two outgoing ω'_1, ω'_2 particle energies. It is convenient to pass to relative momenta \mathbf{k}, \mathbf{k}' and energies ω, ω' and total momentum and energy, \mathbf{q}, Ω . For the on-shell total energy, $\Omega = \omega_1 + \omega_2 = \varepsilon_{k_1} + \varepsilon_{k_2} = 2\varepsilon_k + \varepsilon_q^B$, with the free fermion dispersion relation, $\varepsilon_k = \hbar^2 k^2 / (2m)$, the relative momentum in center-of-mass frame is $k = |\mathbf{k}|$, the center-of-mass momentum is $q = |\mathbf{q}|$ and the free pair dispersion is $\varepsilon_q^B = \hbar^2 q^2 / (2m_B)$ with $m_B = 2m$. The analytically continued, $i\Omega_\nu \rightarrow \Omega + i0^+$, in-medium pair propagator is

$$\chi(\mathbf{k}, \mathbf{q}, \Omega) = \frac{1}{\beta} \sum_{\omega_n} G_0(\xi_+, \Omega) G_0(\xi_-, \Omega - \omega_n), \quad (3)$$

where $\xi_\pm = \varepsilon_{\pm\mathbf{k}+\mathbf{q}/2} - \mu$. We tacitly used the fact that the T-matrix is independent of the relative Matsubara frequencies. Let the two-body limit of the T-matrix be denoted by T_0 and the free two-particle propagator by χ_0 . The corresponding two-body limit of the many-body T-matrix equation then becomes $T_0 = U + U\chi_0 T_0$. The renormalization procedure consists of re-expressing the T-matrix in terms of two-body quantities which on the other hand can be expressed directly in terms of the scattering phase shift of the two-particle wave function in relative coordinates. Heuristically, we may define L from the equation $U = (1 - \chi_0)T_0 \equiv LT_0$ and therefore find $T = L^{-1}LT = L^{-1}(T - \chi_0 T) = L^{-1}U(1 + (\chi - \chi_0)T)$. Hence, after eliminating the bare interaction the T-matrix equation becomes

$$T = T_0 + T_0(\chi - \chi_0)T. \quad (4)$$

The off-shell two-body T-matrix $T_0(k)$ is related to the two-particle off-shell scattering amplitude $f(k)$, as $T_0(k) = -4\pi\hbar^2 f(k)/m = -[g(k) + ik]^{-1}$, where we introduced the relative momentum of the two colliding atoms, $k = \sqrt{mE} = \sqrt{m}(\Omega - \varepsilon_q^B)^{1/2}$ and where

for small momenta the function $g(k) = k \cot \delta_0$ can be expanded in relative energy $\sim \hbar^2 k^2 / m$. Thus, $g(k) = -a_F^{-1} + r_e k^2 / 2 + \dots$, where a_F is the scattering length of the fermions, and r_e is the effective range. The *shape-independent approximation* applied here consists of using only the two first expansion coefficients which characterizes the potential by its depth and range, but is more generally also a valid approximation for multichannel scattering problems. For model potentials the shape dependence is reflected in the signs and magnitudes of the higher order expansion coefficients. The effective range has dimension of length and is for an attractive monotonic potential at resonance, $a_F \rightarrow \pm\infty$, the range of the inter-atomic potential. For the resonance phenomena considered here the effective range can be large and negative. Inserting the low energy expansion of $g(k)$ into the scattering amplitude, $f(k) = k^{-1} e^{i\delta_0} \sin(\delta_0) = (-a_F^{-1} + r_e k^2 / 2 - ik)^{-1}$, the two-body T-matrix becomes, $T_0(k) = -(4\pi a_F / m)(1 - r_e a_F k^2 / 2 - ik)^{-1}$. Adding and subtracting $1/2\varepsilon_{k'}$ in Eq. (4) and using the identity

$$ik = \frac{1}{\mathcal{V}} \sum_{\mathbf{k}'} \left(\chi_0(\mathbf{k}', \mathbf{q}, \Omega) - \frac{1}{2\varepsilon_{k'}} \right), \quad (5)$$

the free two-particle pair propagator, χ_0 , can be eliminated from the problem. After inserting the expression for ik into the Eq. (4) the inverse effective interaction can be defined as

$$U_*^{-1}(k) = -\frac{m}{4\pi\hbar^2} \left(\frac{1}{a_F} - \frac{1}{2} r_e k^2 \right). \quad (6)$$

By solving the T-matrix equation the expression for the inverse T-matrix becomes

$$T^{-1}(\mathbf{q}, \Omega) = (U_*^{-1}(E) - \tilde{\chi}(\mathbf{q}, \Omega)), \quad (7)$$

where the regularized nonzero temperature in-medium pair propagator is,

$$\tilde{\chi}(\mathbf{q}, \Omega) = \frac{1}{\mathcal{V}} \sum_{\mathbf{k}'} \left(\chi(\mathbf{k}', \mathbf{q}, \Omega) - \frac{1}{2\varepsilon_{k'}} \right). \quad (8)$$

The Matsubara sum in $\chi(\mathbf{k}', \mathbf{q}, \Omega)$ is evaluated by turning the sum over Matsubara poles into a contour integral using standard techniques [23]. The regularized pair propagator $\tilde{\chi}$ then becomes

$$\tilde{\chi}(\mathbf{q}, \Omega) = \frac{1}{\mathcal{V}} \sum_{\mathbf{k}'} \frac{1 - n_F(\xi_+) - n_F(\xi_- - \Omega)}{\xi_+ + \xi_- - \Omega} - \frac{1}{2\varepsilon_{k'}} \quad (9)$$

where $n_F(\xi) = (e^{\beta\xi} + 1)^{-1}$ is the Fermi-Dirac distribution function. At a later stage we are going to make a low q, Ω expansion of $\tilde{\chi}$ and therefore keep the Ω in n_F in the numerator [24]. For certain values of β and μ the pair propagator $\tilde{\chi}$ can be calculated analytically, but it is generally evaluated by numerical integration. The angular dependence $x \equiv \cos \theta = \mathbf{k}' \cdot \mathbf{q} / k'q$ is absent

in the denominator and the angular integration can be carried out analytically in the numerator. The regularized pair propagator thus reduces to a one dimensional integral over the magnitude of the relative momentum. After renormalization and making the effective range expansion the equation for the T-matrix is of the same form as in the corresponding equation obtained from the bare contact potential with the only difference being the energy dependence of the effective interaction, $U_* \rightarrow U_*(E)$ where $E = \hbar^2 k^2/m$. Having obtained the expression for the T-matrix the self-energy becomes

$$\Sigma(\mathbf{k}, \omega_n) = \frac{1}{\beta\mathcal{V}} \sum_{\mathbf{q}, \Omega_\nu} T(\mathbf{q}, \Omega_\nu) G_0(\mathbf{q} - \mathbf{k}, \Omega_\nu - \omega_n), \quad (10)$$

where $\Omega_\nu = 2\pi n/\beta$ for integer ν are the bosonic Matsubara frequencies.

To locate the transition temperature we apply the Thouless criterion [25] which states that the transition to the superfluid state is found from the singular behavior of the T-matrix in the long wavelength and low energy limit. At T_c the Thouless criterion is equivalent to the gap equation. For a fixed number of atoms and at the transition temperature the crossover equations are then $T^{-1}(\mathbf{q}, \Omega) = 0$ for $q \rightarrow 0$ and $\Omega \rightarrow 0$ together with the equation for the particle number conservation. In order to calculate the particle number density $n = N/\mathcal{V}$ self-consistently we use the thermodynamic relation, $N = -\partial_\mu \Omega$, where Ω is the grand canonical potential, $e^{-\beta\Omega} = \text{Tr} [e^{-\beta K}]$, tracing over all degrees of freedom. At the transition the result for the normal phase is still valid and the thermodynamic potential can be found from the Luttinger-Ward expression for the grand potential

$$\Omega[G, \Sigma] = \Phi[G] - \frac{1}{\beta\mathcal{V}} \sum_{\mathbf{k}, \omega_n, \sigma} e^{i\Omega_\nu 0^+} [\ln(-G_0^{-1} + \Sigma) + \Sigma G], \quad (11)$$

where the physical dressed Green's function $G(\mathbf{k}, \omega)$ for the atoms and the self-energy $\Sigma(\mathbf{k}, \omega_n)$ are found from the stationary points of Ω with respect to variations of both G and Σ . Here, $\delta\Omega/\delta\Sigma = 0$ yields the Dyson equation Eq. (2) and $\delta\Omega/\delta G = 0$ links the self-energy, Σ , to the functional Φ which is the generating functional for the skeleton graphs and is here constructed in order to generate the ladder approximation by functional differentiation, $\Sigma = \frac{1}{2}\delta\Phi/\delta G$ [26]. In the ladder approximation

$$\Phi = \frac{1}{\beta\mathcal{V}} \sum_{\mathbf{q}, \Omega_\nu} \ln(1 - U_* \chi). \quad (12)$$

A self-consistent treatment of the zero effective range crossover problem has been presented in [21, 27, 28]. We have employed a non-selfconsistent approach where the dressed Green's functions in the pair propagator and the self-energy has been replaced by G_0 and which is equivalent to the functional integral approach of [16]. In this approximation the grand canonical potential takes the form,

$$\Omega = \Omega_0^F + \delta\Omega, \text{ with } \Omega_0^F = \sum_{\mathbf{k}, \omega_n, \sigma} e^{i\omega_n 0^+} \ln G_0(\mathbf{k}, \omega_n)/\beta\mathcal{V} \text{ and } \delta\Omega = \sum_{\mathbf{q}, \Omega_\nu} e^{i\Omega_\nu 0^+} \ln T(\mathbf{q}, \Omega_\nu)/\beta\mathcal{V} \text{ [25].}$$

III. TRANSITION TEMPERATURE

In a BCS superfluid the dispersion relation for the quasiparticle excitations is, $E_{\mathbf{k}} = (\xi_{\mathbf{k}}^2 + \Delta^2)^{1/2}$, and which displays an energy gap, $\Delta \sim U\langle\psi\psi\rangle$, with $\langle\psi\psi\rangle$ being an anomalous thermal correlator. Due to the energy gap in the single particle spectrum thermodynamic and transport quantities, such as the heat capacity and thermal conductivity, may become exponentially suppressed in the superfluid phase and may therefore be used as thermodynamic signatures of the phase transition. Apart from such quantities being difficult to observe directly in a trapped atom gas there are in a strongly interacting Fermi gas additional contributions to the quasiparticle gap which may further complicate the identification of the superfluid transition from such observables. A simple way to see the appearance of such a non-BCS gap contribution at zero temperature is to note that the gap in the quasiparticle spectrum is the minimum of $E_{\mathbf{k}}$ over all \mathbf{k} 's. In the BCS limit the chemical potential is positive and approximately the Fermi energy, and the gap is Δ for $k = k_F$. By contrast when the chemical potential becomes negative on the BEC side the minimum is shifted to $k = 0$ for the gap $(\mu^2 + \Delta^2)^{1/2}$ [14]. The appearance of μ in $E_{\mathbf{k}}$ is related to the molecular degrees of freedom which also contribute to the gap at higher temperatures.

A. Scattering length only

Let us initially consider the zero range limit, $r_e = 0$, which results in the standard BCS to BEC crossover of a Fermi gas with contact interaction [15, 16]. The transition temperature $T_c = 1/\beta_c$ and the chemical potential μ_c are at the transition determined from the Thouless criterion, $\lim_{q, \Omega \rightarrow 0} T^{-1}(\mathbf{q}, \Omega) = 0$, together with the number density equation, $n = n_0^F(\beta, \mu) + \delta n(\beta, \mu)$, where the fermion contribution is $n_0^F(\beta, \mu) = \sum_{\mathbf{k}, \sigma} n_F(\xi_k)/\mathcal{V}$. The fluctuation term δn derived from the ladder self-energy contribution to the thermodynamic potential is $\delta n(\beta, \mu) = -\sum_{\mathbf{q}} \sum_{\Omega_\nu} \partial_\mu \ln T(\mathbf{q}, \Omega_\nu)/\beta\mathcal{V}$. To simplify the calculation of the bosonic number density we follow [16, 24, 29, 30, 31] and make a low energy and long wavelength expansion of the inverse T-matrix

$$T^{-1}(\mathbf{q}, \Omega) = Z(\Omega - \varepsilon_q^B - \mu_B), \quad (13)$$

where $i\Omega_\nu \rightarrow \Omega$ before frequency expansion, the molecular dispersion relation is $\varepsilon_q^B = \hbar^2 \mathbf{q}^2/2m_B^*$ with m_B^* being the renormalized boson mass, the wave function renormalization constant $Z = Z(\beta, \mu)$, the effective boson mass $m_B^* = m_B^*(\beta, \mu)$ and the bosonic chemical potential $\mu_B = \mu_B(\beta, \mu)$ are found from the low order energy and momentum expansion coefficients of $\tilde{\chi}$ together

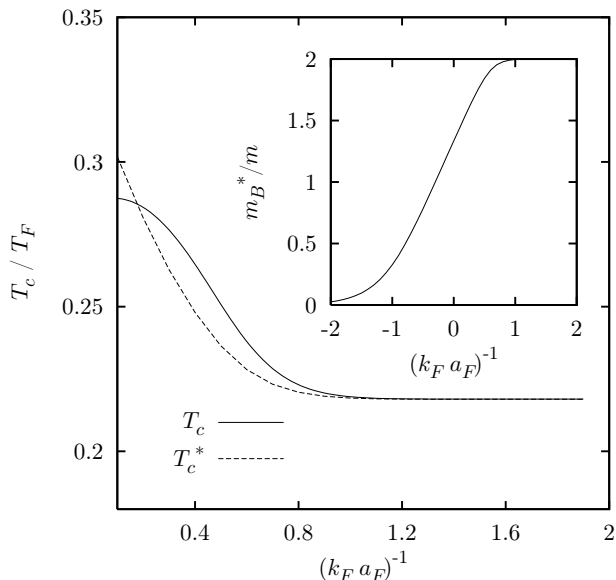


Figure 2: The transition temperature for $r_e = 0$ on the BEC side of the crossover is plotted as a function of the inverse coupling constant from the full calculation (full curve) and the corresponding result (dashed curve) obtained from the expression for the transition temperature for the non-interacting BEC with the numerically calculated effective boson mass. The inset shows the crossover behavior of the effective boson mass in units of the fermion mass in the whole crossover region.

with $U_*^{-1}(k)$. Re-expressing the frequency integration as a standard sum over bosonic Matsubara frequencies δn becomes

$$\delta n(\beta, \mu) = \frac{1}{\mathcal{V}} \sum_{\mathbf{q}} n_B(\xi_q^B) (-\partial_\mu \xi_q^B), \quad (14)$$

where $\xi_q^B = \varepsilon_q^B - \mu_B$, and $n_B(\xi) = (e^{\beta\xi} - 1)^{-1}$ is the Bose-Einstein distribution function.

Before we turn to the results of the numerical calculations we note that the results for the uniform case with a contact potential are well-known: In the weak coupling limit as $(k_F a_F)^{-1} \rightarrow -\infty$ the Fermi gas is expected to make a transition at the transition temperature $T_c = (8e^{\gamma-2}/\pi) T_F e^{-\pi/2k_F|a_F|}$ to a pair-correlated BCS-state, where the Fermi temperature is, $T_F = E_F/k_B$, and $\gamma = 0.57721\dots$ is the Euler-Mascheroni constant. For a uniform noninteracting two-component Fermi gas with the Fermi energy E_F the corresponding Fermi wave vector is $k_F = (2mE_F/\hbar^2)^{1/2}$, and the particle density is $n = k_F^3/3\pi^2$. As the inverse scattering length is increased strong coupling effects appear and when $(k_F a_F)^{-1}$ passes through zero from below a two-body bound (molecular) state appears, and the fermionic states hybridize with the molecular states. When the inverse scattering length is increased further $(k_F a_F)^{-1} \rightarrow \infty$ the Fermi surface smears out (which can be seen by inspection of the momentum distribu-

tion) and a molecular Bose gas is formed which undergoes Bose-Einstein condensation at the transition temperature $T_{BEC} = (\hbar^2/2mk_B)2\pi\zeta(3/2)^{-2/3}(n/2)^{2/3} \approx 0.218T_F$. Between the two limits the system smoothly crosses from BCS-like behavior to BEC-like behavior in the region, $-1 \lesssim (k_F a_F)^{-1} \lesssim 1$. In the BEC limit where the fermion contribution vanishes δn reduces to twice the boson density obtained from the Bose-Einstein distribution, $\delta n(\beta, \mu) = 2 \sum_{\mathbf{q}} n_B(\xi_q^B)/\mathcal{V}$, for bosons with the mass twice that of the atoms, $m_B^* = m_B = 2m$.

The problem of numerically solving the pair of equations $n = n_0 + \delta n$ and $T^{-1}(\mathbf{0}, 0) = 0$ for β_c and μ_c was solved iteratively using multidimensional root solvers implemented in [32]. At each iteration the momentum integrals appearing in $Z, m_B^*, \delta n, \mu_B$ and in the μ derivatives appearing in the number equation were numerically integrated using appropriate adaptive quadrature algorithms [33] also reimplemented in [32]. The numerical results for the zero effective range crossover are presented in Fig. 3 (full curve) and show a smooth crossover with characteristic T_c peak near the zero of the chemical potential and qualitatively in agreement with previous calculations [15, 16].

For a weakly interacting Bose gas there are a number of corrections due to critical fluctuations close to T_c with the leading term being linear and positive in the bosonic gas parameter $\propto k_F a_F$ and indicating a peak in T_c . Mean field corrections to the transition temperature for a weakly interacting Bose gas with nonzero effective range give rise to a leading correction term which is negative and cubic in the gas parameter and thus indicates absence of peak in T_c . However, the non-selfconsistent Gaussian model presented here includes none of the above mentioned boson-boson effects and the correction to T_c observed on the BEC side here is due to an externally induced change of the molecular binding energy E_0 . When $(k_F a_F)^{-1}$ is lowered by increasing the strength of the effective interaction the binding energy goes down and the molecules dissociate more easily at a fixed temperature and in addition the fermion states become populated. The coupling to the fermions also gives rise to a renormalized boson mass, $m_B^* < m_B$, where the bare boson mass is $m_B = 2m$. Therefore the ideal Bose gas condensation temperature is shifted to higher values, $T_c = T_{BEC} + \delta T_{BEC}$ where $\delta T_{BEC}/T_{BEC} \propto |\delta m_B|/m_B$ for decreasing effective mass, $\delta m_B = m_B^* - m_B$ as $(k_F a_F)^{-1}$ increases. In Figure 2 the transition temperature in the BEC limit is plotted as a function of the $(k_F a_F)^{-1}$ using the numerically calculated T_c (full curve) and using the ideal Bose gas expression for the transition temperature with $T_c^* \equiv T_{BEC}^* \propto 1/m_B^*$ using the numerically calculated effective mass m_B^* . The inset in Figure 2 shows the effective mass m_B^* identified from the asymptotic behavior of the T-matrix, see Eq. (13). The effective mass becomes as expected twice the fermion mass in the BEC limit, but no attempt was made to decompose δn into partial contributions. Thus, the effective boson mass becomes a hybrid object in the crossover region

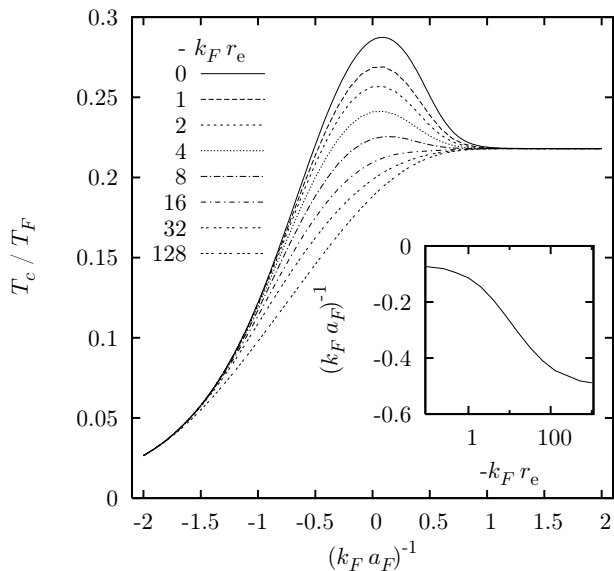


Figure 3: The BCS-BEC crossover transition temperature of the homogeneous Fermi gas as a function of the inverse coupling constant, $-2 \leq (k_F a_F)^{-1} \leq 2$, for several values of the effective range parameter $k_F r_e$. The zero range result (full curve) corresponds to the usual T_c curve for the crossover. For increasing values of the $-k_F r_e$ the transition temperature is suppressed in the crossover region. In the inset we characterize the small effective range to large effective range crossover by plotting the half-density crossing point in $(k_F a_F)^{-1}$ as a function of the $-k_F r_e$. The curve shows a shift in the position of the crossing to lower couplings for increasing $-r_e$.

without clear physical interpretation as a single particle mass.

B. Effective range expansion

As indicated in the introduction narrow Feshbach resonances can be mimicked by an interaction potential with large and negative effective range. To account for such a situation the zero effective range contact potential must be replaced by a potential with nonzero range. However, for monotonic and attractive potentials the effective range is at resonance the averaged microscopic range of the potential and thus positive [34]. For potential models the effective range can be related to the structure of the interaction potential and can be negative in the presence of repulsive cores or barriers. In the latter case considered here the negative effective range is related to the resonance physics of potentials with barriers. For a potential with a barrier quasi-bound states may appear which have a finite lifetime and thus decay into the continuum states. In the zero temperature calculation [17, 35] it was suggested to mimic the presence Feshbach resonances by using a two-body square well with a square barrier model potential in place of the contact potential. In contrast we use the renormalized crossover equations of Section

II and the numerics of subsection III A to examine the effect of the energy dependent effective interaction

$$U_*(k) = -\frac{4\pi a_F}{m} \left(1 - \frac{1}{2} r_e a_F k^2\right)^{-1} \quad (15)$$

on the transition temperature for values of the effective range $-k_F r_e$ ranging from small to large and positive.

In Figure 3 the numerical results for the transition temperature for several values of $-k_F r_e = 1, 2, 4, 8, 16, 32, 128$ are plotted as a function of the $(k_F a_F)^{-1}$ together with the zero range $r_e = 0$ result (full curve). For a broad resonance with vanishing $k_F r_e$ the usual zero effective range result is obtained. In the crossover region the transition temperature is sensitive to the effective range and the peak in T_c becomes suppressed for increasing values of $-k_F r_e$. In the BCS (BEC) limit a negative r_e shifts the effective interaction to lower (higher) values corresponding to a lower transition temperature which is consistent with the decrease in T_c for increasing $-r_e$ at fixed a_F . Furthermore, it is seen that the energy dependence of the effective interaction is only important in the crossover region for $-k_F r_e \gtrsim 1$. The small value of the parameter $(k_F a_F)(k_F r_e)$ the energy dependence of U_* is suppressed and therefore both the asymptotic BCS and BEC limits are recovered even for large $k_F r_e$.

It is tempting to compare our result to the corresponding calculation of T_c for the atom-molecule Hamiltonian. In [36, 37] the transition temperature was calculated as a function of the detuning ν for a homogeneous Fermi gas both for weak inter-channel coupling $g_{BF} = 0.6E_F$ and for strong coupling $g_{BF} = 20E_F$. In addition to an explicit contribution to the number equation arising from the bosonic degrees of freedom, the effective interaction appearing in the Thouless criterion also includes the effect of repeated fermion-boson scattering in addition to the fermion-fermion scattering, $U_*(\mathbf{q}, \Omega_\nu) = U_{FF} - g_{BF}^2 D_0(\mathbf{q}, \Omega_\nu)$, where U_{FF} is the inter-fermion coupling strength, g_{BF} is the boson-fermion coupling strength, $D_0^{-1}(\mathbf{q}, \Omega_\nu) = (i\Omega_\nu - \xi_q^B)^{-1}$ is the free molecule propagator, $\xi_q^B = \hbar^2 q^2 / (2m_B) - 2(\mu - \nu)$ is the bare molecule dispersion relation. For small couplings corresponding to a large and negative effective range T_c was found to increase monotonically from the BCS to the BEC limit. In the opposite limit of large couplings corresponding to a small effective range a pronounced peak close to threshold appears. These results are consistent with the trends found in the present calculation. It is also interesting to compare the result to the transition temperature obtained for a mixture of fermions and long-lived bosons (narrow resonance case) with the total density constrained by total fermion number conservation, and with $m_B = 2m$. By decomposing the total density into three contributions, $n = n_0^F + 2n_0^B + \delta\tilde{n}$, and by neglecting $\delta\tilde{n}$ when solving the crossover equations, a monotonically increasing T_c is found which appears to be the T_c curve in the large $-r_e$ limit. The effective range induce a cutoff in the momentum integrations and thus

reduces the influence of high momentum modes. This decreases the effect of the fluctuations and leads to a suppression of T_c which is again consistent with the interpretation of the large T_c peak being due to Gaussian fluctuations. To characterize the 'crossover' from small r_e behavior to large r_e behavior we notice that at a fixed $k_F a_F$ the fermion contribution to the total density becomes suppressed for increasing $-r_e$ due to decrease in the chemical potential in the crossover region. Therefore, the half-density crossing point of the partial densities, $n_0^F = \delta n = \frac{1}{2}$, is shifted to the BCS side. The inset in Fig. 3 shows a semilogarithmic plot of the half-density crossing point as a function of $k_F r_e$. As value of the effective range is increased the crossing point shifts from $(k_F a_F)^{-1} \approx -0.07$ for $r_e = 0$ to $(k_F a_F)^{-1} \approx -0.5$ in the large $-r_e$ limit where the dependence on the effective range is expected to drop out. Therefore, the transition temperature appear to have a lower bound at fixed coupling for large $-r_e$ when neglecting high order terms in the expansion of $k \cot \delta$.

It is to be noted that the current calculation does not account for i) the induced interactions due to vertex corrections which reduce T_c by a factor of 2.2 in the BCS limit [38]. ii) the residual boson-boson and boson-fermion interactions which are characterized by the boson-boson scattering length, a_B , and the boson-fermion scattering length, a_{BF} , on the BEC side as recently found from solving three and four-body problems [39]. Let us finally mention that to the extent that many-body physics is important to the crossover problem it must be stressed that many theoretical issues, e.g., non-zero effective range calculations, renormalization of coupling constants, inclusion of higher order diagrammatic contributions, and

generalization to pairing states in higher angular momentum channels, are easier to handle within the single channel potential model.

IV. SUMMARY

We presented the renormalized T-matrix equation which allowed the non-zero effective range BCS-BEC crossover equations at the transition to be formulated directly in terms of two-body scattering properties, the scattering length and the effective range. By matching the scattering properties of the generalized single-channel BCS-BEC crossover model with the two-channel Feshbach resonance atom-molecule model it was argued that the internal energy scale of a resonance translates into to the effective range of the potential model. Broad resonances correspond to a small effective range and for narrow resonances the effective range become large and negative. By using the NS crossover equations with the self-energy derived from the ladder approximation we numerically calculated the superfluid transition temperature of the generalized BCS-BEC crossover model as a function of the two-body scattering length and found T_c to be suppressed in the crossover region for increasing values of $-k_F r_e$.

Acknowledgments

It is a pleasure to acknowledge helpful discussions with Chris Pethick.

-
- [1] C. A. Regal, C. Ticknor, J. L. Bohn, and D. S. Jin, *Nature* **424**, 47 (2003).
 - [2] J. Cubizolles, T. Bourdel, S. J. J. M. F. Kokkelmans, G. V. Shlyapnikov, and C. Salomon, *Phys. Rev. Lett.* **91**, 240401 (2003).
 - [3] K. E. Strecker, G. B. Partridge, and R. G. Hulet, *Phys. Rev. Lett.* **91**, 080406 (2003).
 - [4] S. Jochim, M. Bartenstein, A. Altmeyer, G. Hendl, C. Chin, J. H. Denschlag, and R. Grimm, *Science* **302**, 2101 (2003).
 - [5] M. Greiner, C. A. Regal, and D. S. Jin, *Nature* **426**, 637 (2003).
 - [6] W. Zwiernlein, C. Stan, C. Schunck, S. M. F. Raupach, S. Gupta, Z. Hadzibabic, and W. Ketterle, *Phys. Rev. Lett.* **91**, 250401 (2003).
 - [7] M. Bartenstein, A. Altmeyer, S. Riedl, S. Jochim, C. Chin, J. H. Denschlag, and R. Grimm, *Phys. Rev. Lett.* **92**, 120401 (2004).
 - [8] M. Bartenstein, A. Altmeyer, S. Riedl, S. Jochim, C. Chin, J. H. Denschlag, and R. Grimm, *Phys. Rev. Lett.* **92**, 203201 (2004).
 - [9] C. A. Regal, M. Greiner, and D. S. Jin, *Phys. Rev. Lett.* **92**, 040403 (2004).
 - [10] M. Zwiernlein, C. A. Stan, C. H. Schunck, S. F. Raupach, A. J. Kerman, and W. Ketterle, *Phys. Rev. Lett.* **92**, 120403 (2004).
 - [11] C. Chin, M. Bartenstein, A. Altmeyer, S. Riedl, S. Jochim, J. H. Denschlag, and R. Grimm, *Science* **305**, 1128 (2004).
 - [12] J. Kinnunen, M. Rodríguez, and P. Törmä, *Science* **305**, 1131 (2004).
 - [13] J. Kinast *et al*, *Phys. Rev. Lett.* **92**, 150402 (2004).
 - [14] A. J. Leggett, in *Modern Trends in the Theory of Condensed Matter* (Springer Verlag, 1980), p. 13.
 - [15] P. Nozières and S. Schmitt-Rink, *J. Low Temp. Phys.* **59**, 195 (1985).
 - [16] C. A. R. Sá de Melo, M. Randeria, and J. R. Engelbrecht, *Phys. Rev. Lett.* **71**, 3202 (1993).
 - [17] S. De Palo, M. L. Chiofalo, M. J. Holland, and S. J. J. M. F. Kokkelmans, *Physica A* **327**, 490 (2004).
 - [18] G. M. Bruun and C. J. Pethick, *Phys. Rev. Lett.* **92**, 140404 (2004).
 - [19] R. Diener and T.-L. Ho, *cond-mat/0405174* (2004).
 - [20] S. Simonucci, P. Pieri, and G. C. Strinati, *cond-mat/0407600* (2004).
 - [21] R. Haussmann, *Z. Phys. B* **91**, 291 (1993).

- [22] D. M. Eagles, Phys. Rev. **186**, 456 (1969).
- [23] A. L. Fetter and J. D. Walecka, *Quantum Theory of Many-Particle Systems* (McGraw-Hill, Inc., 1971).
- [24] J. Quintanilla, B. L. Gyorffy, J. F. Annett, and J. P. Wallington, Phys. Rev. B **66**, 214526 (2002).
- [25] D. J. Thouless, Ann. Phys. **10**, 553 (1960).
- [26] G. Baym, Phys. Rev. **127**, 1391 (1962).
- [27] R. Haussmann, Phys. Rev. B **49**, 12975 (1994).
- [28] R. Haussmann, *Self-consistent Quantum-Field Theory and Bosonization for Strongly Correlated Electron Systems* (Springer-Verlag, New York, 1999).
- [29] M. Drechsler and W. Zwerger, Ann. Phys. **1**, 15 (1992).
- [30] S. Stintzing and W. Zwerger, Phys. Rev. B **56**, 9004 (1997).
- [31] Q. Chen, I. Kosztin, B. Jankó, and K. Levin, Phys. Rev. Lett. **81**, 4708 (1998).
- [32] M. Galassi *et al.*, *GNU Scientific Library Reference Manual* (Network Theory Ltd., Bristol, 2003), 2nd ed.
- [33] R. Piessens *et al.*, *QUADPACK, A Subroutine Package for Automatic Integration* (Springer Verlag, 1983).
- [34] J. M. Blatt and J. D. Jackson, Phys. Rev. **76**, 18 (1949).
- [35] R. B. Diener and T.-L. Ho, cond-mat/0404517 (2004).
- [36] Y. Ohashi and A. Griffin, Phys. Rev. Lett. **89**, 130402 (2002).
- [37] Y. Ohashi and A. Griffin, Phys. Rev. A **67**, 033603 (2003).
- [38] L. P. Gorkov and T. K. Melik-Barkhudarov, JETP **13**, 1018 (1961).
- [39] D. Petrov, C. Salomon, and G. Shlyapnikov, cond-mat/0407579 (2004).